Available online at www.sciencedirect.com
ScienceDirect
Computers, Environment and Urban Systems 32 (2008) 317–326
Computers, Environment and Urban Systems
www.elsevier.com/locate/compenvurbsys

Classification of the wildland–urban interface: A comparison of pixel- and object-based classifications using high-resolution aerial photography

Casey Cleve [a,*], Maggi Kelly [b], Faith R. Kearns [a], Max Moritz [a]

[a] Center for Fire Research and Outreach, University of California, Berkeley, 137 Mulford Hall #3114, Berkeley, CA 94720, United States
[b] Geospatial Imaging and Informatics Facility, University of California, Berkeley, 137 Mulford Hall #3114, Berkeley, CA 94720, United States

Received 21 June 2007; received in revised form 5 October 2007; accepted 8 October 2007

Abstract

The expansion of urban development into wildland areas can have significant consequences, including an increase in the risk of structural damage from wildfire. Land-use and land-cover maps can assist decision-makers in targeting and prioritizing risk mitigation activities, and remote sensing techniques provide effective and efficient methods to create such maps. However, some image processing approaches may be more appropriate than others in distinguishing land-use and land-cover categories, particularly when classifying high spatial resolution imagery for urbanizing environments. Here we explore the accuracy of pixel-based and object-based classification methods used for mapping in the wildland–urban interface (WUI) with free, readily available, high spatial resolution urban imagery, which is available in many places to municipal and local fire management agencies. Results indicate that an object-based classification approach provides a higher accuracy than a pixel-based classification approach when distinguishing between the selected land-use and land-cover categories. For example, an object-based approach resulted in a 41.73% greater accuracy for the built area category, which is of particular importance to WUI wildfire mitigation.

Keywords: Wildland–urban interface; Classification; Image analysis; Object-based methods; Remote sensing

1. Introduction

The increased proximity between developed and wildland areas that often accompanies new development places people and homes at risk from wildfire. In California alone, over five million homes are located in wildland–urban interface (WUI) areas (Radeloff et al., 2005) and that number is likely to grow as the state population continues to increase. Accurate and timely land-use and land-cover (LULC) maps are needed for wildfire management; maps are needed before fires happen to model potential risk, during fires to assist fire safety personnel in fire-fighting and evacuation, and after fires to better mitigate the ecological consequences of fire. In all cases, it is important to accurately distinguish homes and other features of the built environment from vegetation across a large geographic extent. The location of a structure, and its arrangement relative to other structures or flammable materials, is of key interest in preventing wildfire-related losses in the WUI (Cohen 2000; Frontiera & Kearns 2007; Murname 2006).

Over regional scales, LULC maps are typically produced from remotely sensed image analysis using moderate resolution satellite imagery such as Landsat TM (Alberti et al., 2004; Cihlar, 2000; Hollister et al., 2004; Vogelmann et al., 1998, 2001; Walsh et al., 2001). While these products are useful for producing coarse-scale classifications, they are inadequate for detailed mapping (e.g., species-level vegetation or buildings) (Harvey & Hill, 2001; Kalliola & Syrjänen, 1991). LULC maps of urban environments require finer detail, and utilize either photointerpretation

* Corresponding author. Tel.: +1 510 643 0409; fax: +1 510 643 3490.
E-mail address: caseycleve@gmail.com (C. Cleve).

0198-9715/$ - see front matter © 2007 Elsevier Ltd. All rights reserved.
doi:10.1016/j.compenvurbsys.2007.10.001

or image processing of high-resolution aerial photographs (Bauer & Steinnocher, 2001; Benediktsson et al., 2003; Ehlers et al., 2003; Herold, Gardner, et al., 2003; Jensen & Cowen, 1999; Kettig & Landgrebe, 1976). Freely available, high spatial resolution aerial imagery is increasingly accessible to municipal governments, fire management agencies, and communities. In the US in particular, state and local governments are acquiring high spatial resolution imagery to monitor everything from invasive species to development patterns and making them freely available to users. These images can be an important resource, particularly for the often under-funded and under-staffed state and local agencies charged with wildfire mitigation in the WUI (Thomas et al., 2003). However, photointerpretation, particularly over large areas, is labor-intensive, subjective, and often expensive. Therefore, it is important to develop image-processing techniques that at least partially automate the process of classifying high-resolution aerial imagery.

While high spatial resolution remote sensing provides more information than coarse resolution imagery for detailed mapping, increasingly finer spatial resolution produces challenges for classic pixel-based techniques such as Iterative Self-Organizing Data Analysis Technique (ISODATA) and Maximum Likelihood Classifier (MLC); these methods assume individual pixels on each image are independent, and they are treated in the classification algorithm without considering any spatial association with neighboring pixels. With high spatial resolution imagery, single pixels no longer capture the characteristics of classification targets (Yu et al., 2006). Instead, adjacent pixels tend to belong to the same class or some compatible classes with an ecological or functional association (Liu et al., 2006). The increase in intra-class spectral variability reduces statistical separability between classes and classification accuracy is reduced (Yu et al., 2006). The classification results often show a "salt-and-pepper" effect, with individual pixels classified differently from their neighbors (Kelly et al., 2004).

"Object-based" classifiers can be used to overcome these problems by first segmenting an image into clusters of similar neighboring pixels ("objects"), and then classifying the clusters according to average (or other) spectral properties. This reduces local spectral variation within objects, and allows for other contextual and topological relationships (e.g., "close to", "surrounded by", "next to") to be utilized in the classification process. Image objects are therefore basic entities in an image (in our case, roofs, roads, vegetation, etc.), where each pixel group is composed of similar digital values, and possesses an intrinsic size, shape, and geographic and/or ecological relationship within the real-world scene component it models (Hay et al., 2001). While this idea has been around for some time (e.g., Kettig & Landgrebe, 1976), computational power and software advancements are now making widespread use of this approach more feasible.

Numerous researchers have used these methods to successfully map features with distinct spatial boundaries (Barlow et al., 2003, 2006; Zhang et al., 2005). For example, Barlow et al. (2003) used image segmentation and classification to identify landslide scars in the Cascade Mountains in British Columbia using panchromatic SPOT imagery. Zhang et al. (2005) developed a segmentation method for classifying burn scars using NDVI differenced SPOT imagery. Others have reported using object-based classification to map vegetation species or structure in high spatial-resolution imagery with more detail than conventional pixel-based methods (Chubey, et al., 2006; Laliberte et al., 2004; Yu et al., 2006).

These methods have been particularly successful in urban environments. Herold, Liu, et al. (2003) used object-based methods to map urban land use in California using Ikonos imagery; they argue that spatial resolutions better than 5 m are required for such mapping. Thomas et al. (2003) compared traditional pixel-based classification methods in an urban environment with two methods that incorporated shape, texture, and context in the process; the first was a time-consuming manual raster modeling approach, the second was an object-based classification. The raster model outperformed the other methods, but the near automated object-based classification method was a close second.

Here we evaluate both an object-based classification approach and a conventional pixel-based classification approach for their value in creating an accurate and near automated classification of, and differentiation between, four urban land-use/land-cover categories that are particularly important for wildfire mitigation and modeling purposes – built areas (structures and transportation), surface vegetation (grassland, irrigated lawns, urban landscaping, and agriculture), trees/shrubs, and shadows. The surface vegetation category is a composite class, because both urban landscaping and agriculture contain a combination of bare area and surface vegetation. The shadow class alone is not particularly valuable; however, it can be used to assist with further class discrimination, such as separating trees from shrubs. The three primary categories (built areas, surface vegetation, and trees/shrubs) are the building blocks of a basic WUI LULC map designed to assist fire management, and rapid, accurate and inexpensive map production is often a basic goal for WUI areas. We mapped all four categories using a freely available 15 cm spatial resolution digital aerial photograph (RGB) for a WUI area in northern California and both pixel-based and object-based mapping approaches. An accuracy assessment was conducted on both maps and these results are compared.

2. Methods

2.1. Study area

This study was conducted in a small community (Deerpark – approximately 1 square mile) in Napa County, California (USA) (Fig. 1). This community was chosen because it is located in the wildland–urban interface area,

Fig. 1. Deerpark community in Napa County (northern California, USA).

and is consequently at risk from wildfire. In addition, it was of interest to the county fire department to map this particular community; local fire departments often have a good idea of areas that might be at risk in a wildland fire situation and are searching for better maps and other information on those locations. Additionally, this area exhibits a variety of land-use and land-cover types characteristic of the region, providing an ideal location to test methods that could be more broadly applied. No urban LULC map exists for this area at this level of detail; however, free high spatial resolution imagery was available.

2.2. Image pre-processing

The imagery analyzed was provided by Napa County and consists of 15cm spatial resolution color aerial photographs acquired on February 23, 2005. The image size was 12000 columns and 8000 rows, covering an area of 1.10 miles by 0.75 miles. Using a relatively small image size such as this is essential when determining the best classification methodology because of the increase in processing speed. Although this area does not cover the entire WUI in Napa County, once appropriate the methodology was determined it could be applied to the entire wildland–urban interface in Napa County. The photographs were georeferenced and orthorectified by Tucker & Associates. Orthorectification was preformed using a Digital Terrain Model provided by Napa County.

Due to the low spectral resolution and high spatial resolution of the image, classifying the 3-band image alone resulted in high confusion between classes. Therefore, spectral and spatial enhancements were explored to increase map accuracy. Mean focal analysis was used to decrease contrasts and emphasize homogeneous information within each class. Two iterations of a (7×7) focal filter were performed on the first principal component containing 95% of the total variance. The first principal component compresses the main information that exists within all three

bands (Jensen & Cowen, 1999). This enhancement combination was chosen because it improved the visual separation of our four target classes (built areas such as structures and transportation, surface vegetation, trees/shrubs, and shadows). This layer was then stacked with the 3-band aerial photograph and used in both the pixel-based and object-based classification approaches (Fig. 2).

2.3. Iterative self-organizing data analysis technique (ISODATA) clustering at the pixel level

The unsupervised classification process ISODATA was run on the combined, spatially-enhanced first principal component and 3-band aerial imagery using Leica Erdas Imagine 8.7. ISODATA is a standard unsupervised classifier (Jensen, 1996; Liu et al., 2006) that uses minimum spectral distance to assign a cluster for each candidate pixel through a number of iterations (Kettig & Landgrebe, 1976). The user specifies a convergence threshold, number of desired classes, and number of iterations. Iterations cease when either the convergence threshold or the maximum number of iterations is reached. The method is not completely automated, as it requires that the analyst manually label the resultant spectral classes to information classes. In our case, 100 clusters were specified, with 20 iterations and a convergence threshold of 0.95. After clustering, the classes were combined into the four target classes. The final classified map was filtered using a 3×3 majority filter in ESRI ArcGIS 9 (ESRI, 2004) to remove spurious pixels common in pixel-based classification approaches (Fig. 3).

2.4. Object-based classification

The first step in an object-based classification approach is image segmentation, which creates image-objects that represent meaningful entities (e.g., roofs or vegetation patches) by grouping adjacent pixels with similar characteristics. Humans can visually group similar pixels into meaningful objects based on the spatial arrangement and pixel color (Hay et al., 2003). Segmentation acts to mimic this behavior by both creating meaningful image-objects and providing object topology (Hay et al., 2003).

All object-based analysis was conducted using Definiens eCognition software (Definiens, 2005). Definiens eCognition software uses a bottom-up segmentation approach, starting with single pixels as separate objects and merging them into larger segments with each iterative step (Baatz et al., 2000). This process is based on image spectral and textural characteristics and user-defined parameters that influence the image-object shape and size. A scale parameter is used to control the size of the image-object – the larger the scale parameter value, the larger the image-object – and a shape criterion is used to influence the smoothness and compactness of the image-object (Baatz et al., 2000). Once segmented, image-objects are populated with spectral and shape statistics, texture parameters, and topological information (Baatz et al., 2000). Here, we segmented the combined, spatially-enhanced first principal component and 3-band aerial image into two different scales of image objects: one that targeted large vegetation patches (large image-objects), and another optimized for small features such as structures (small image-objects) (Fig. 4). After exploring numerous scale and shape parameters, the following were chosen based on how clearly they defined small and large object boundaries: (1) large image-objects were created with a scale parameter of 250 and a shape criterion of 0.239, and (2) small image-objects were created with a smaller scale parameter of 100 and a shape criterion of 0.239.

The segmented image was classified using a combination of fuzzy and nearest neighbor supervised classification techniques. The Definiens eCognition program contains two image classification methods – nearest neighbor (NN) supervised classification and user-defined fuzzy classification (Baatz et al., 2000). Nearest neighbor classification is based on minimum distance and relies on training data to classify the image based on spectral, shape, and/

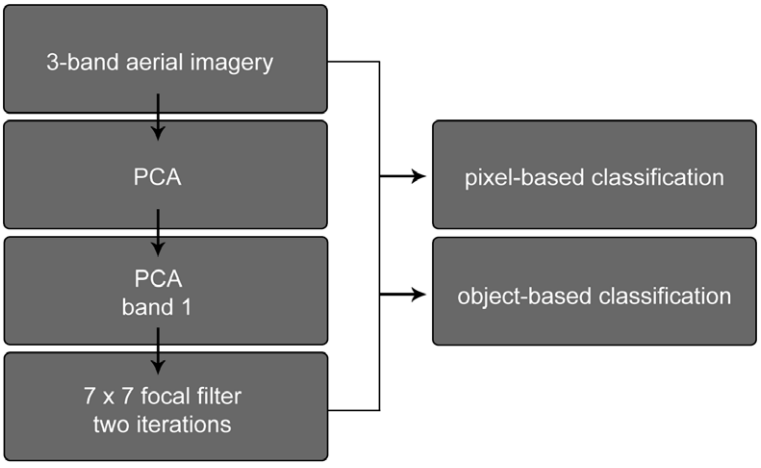

Fig. 2. Flowchart displaying the image pre-processing steps and inputs to the two classification methods.

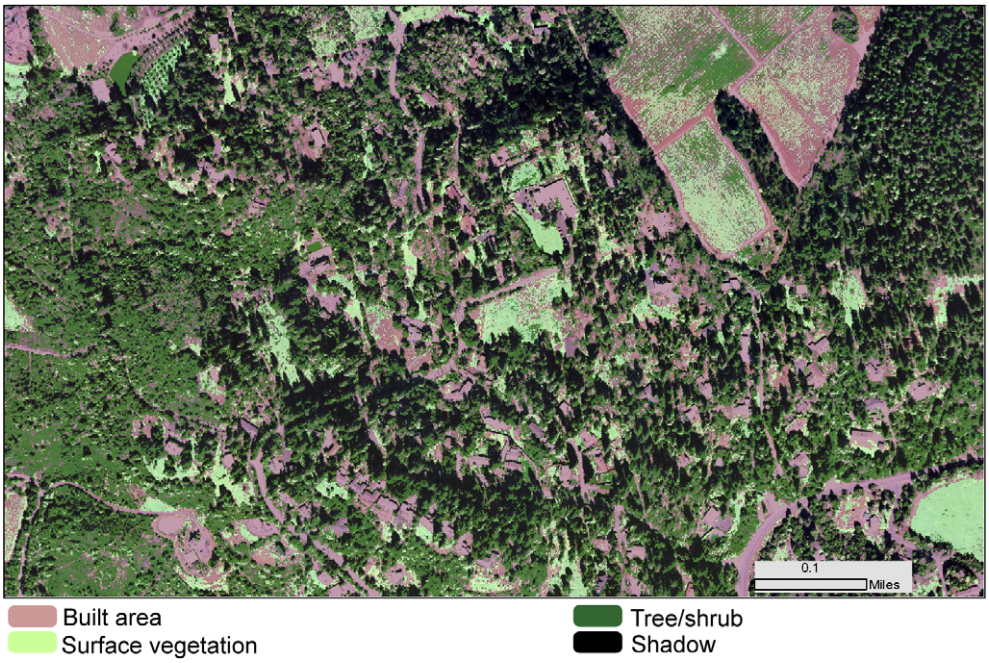

Fig. 3. Final pixel-based classified map.

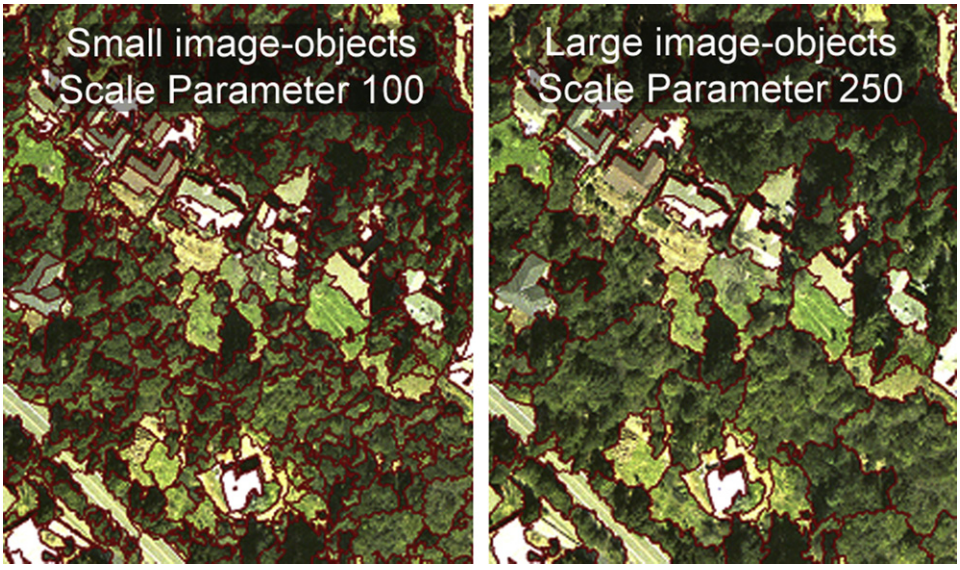

Fig. 4. The left panel displays the small image-objects, while the right panel displays the large image-objects. The small image-object delineate target features such as structures, whereas the large image-objects outline features such as vegetation patches.

or texture feature values. The fuzzy classification method allows the user to convert the range of feature values into fuzzy membership values between 0 and 1, where 1 indicates complete membership in a particular class (Definiens, 2005). To be classed correctly, categories frequently need more than one membership expression, which can be combined using operators such as "and", "or", and "not". The fuzzy classification in Definiens eCognition is not a wall-to-wall classifier; it does not classify every pixel of the image. Each class is extracted individually until the entire image is classified (Baatz et al., 2000).

Multi-scale classification was used to classify the segmented image. First, 90% percent of the image was classified on the large image-object scale using fuzzy class descriptions, which included texture, brightness, and image-object shape and size characteristics. The Feature View tool in Definiens eCognition was used to identify which features and feature value ranges were suitable to map each LULC category (Definiens, 2005). A total of six features were selected for classification (Table 1).

The sole feature chosen for built area extraction was the gray level co-occurrence matrix (GLCM) 'dissimilarity in

Table 1
Per class fuzzy membership feature selection

Built area	Surface vegetation	Tree/shrub	Shadow
Texture: GLCM dissimilarity (all directions), on spatially enhanced first PC	Area of sub-object (small object): Mean	Brightness	Brightness
	Area	Ratio to scene: spatially enhanced first PC	
	Length/width		

all directions' on the spatially-enhanced first principal component. GLCM is a calculation of the frequency of different gray level pixel combinations that occur in the image layer, and GLCM dissimilarity is a measure of the total variation present in each image object (Baatz et al., 2000). Higher values exist if the image object contains a large amount of variation (Baatz et al., 2000). With the spatially-enhanced first principal component, the built areas contained the least amount of variation, making it possible to extract this class by using a fuzzy membership that captured the lowest 20% of the total GLCM value range.

The surface vegetation category was extracted using the relationship between large and small image-objects, specifically the mean area of small image-objects to each large image-object. Using this relationship between large and small image-objects for the surface vegetation class was optimal because, compared to the three other classes, there was a unique relationship between small and large image-objects. At the large image-object scale, the surface vegetation polygon size was similar to that of the other LULC categories. However, at the small image-object scale, surface vegetation polygon size was generally larger than the other classes. Although it wasn't consistently larger, the mean area of small image-objects per large image-object was consistently larger with surface vegetation, making it an ideal membership to use to extract surface vegetation (Fig. 5). This membership was combined with two shape features, which included area and length/width.

Brightness was used to extract both the tree/shrub class and the shadow class. Brightness is the sum of each image-object's spectral mean divided by the number of spectral bands (Baatz et al., 2000). The shadow class, containing the darkest objects, was extracted using the lowest 35% (values 0–95) of the entire brightness range (0–255). The tree/shrub category, the second darkest class, was extracted using the next 35% (values 95–130) of the entire brightness range. Due to spectral variability present in the shrub/tree class, one additional feature membership was needed to classify it – the spatially enhanced first principal component ratio to scene per image object. This feature is the image object's mean value of the spatially enhanced first principal component layer divided by this layer's scene mean value. This feature captured light green trees and shrubs that the brightness feature was unable to extract.

The large image-object scale could only be used to classify 90% of the image because this segmentation scale was too large to classify all small features accurately. Therefore, the small image-object scale was used to separate these features and to classify the remaining 10% of the image. The classified large image-objects were applied to small image-objects using the 'existence of' fuzzy membership function. Then the remaining 10% of the image was classified using nearest neighbor supervised classification with 20 photointerpreted samples for training data (Fig. 6).

2.5. Accuracy assessment

Classification accuracy was measured for both classification methods using a standard error matrix, and matrices were compared using a pairwise z-score significance test (Congalton & Green, 1999) (Table 2). We purposefully used identical error assessment techniques to evaluate the pixel- and object-based classifications. The same reference points visually interpreted from the original imagery, con-

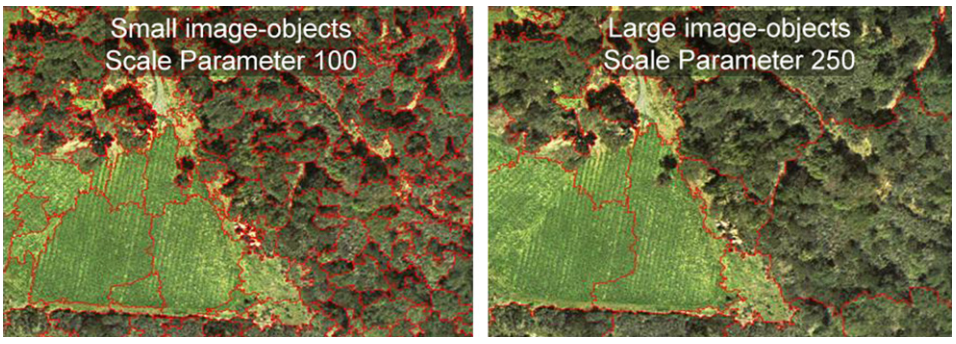

Fig. 5. There is a unique size relationship between small and large image-objects for surface vegetation. Surface vegetation image-object size was larger in the small image-object scale compared to the other categories, but at the large image-object scale it was generally the same size as the other categories.

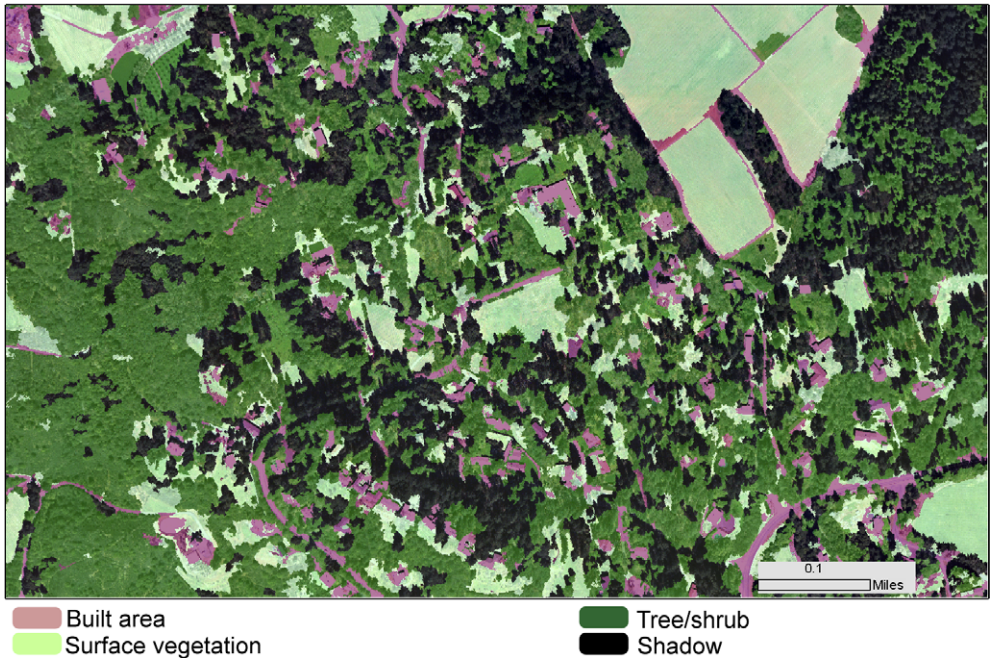

Fig. 6. Final object-based classified map.

Table 2
Accuracy matrices for pixel-based and object-based classification methods

Classified	Reference					
	Built area	Surface vegetation	Tree/shrub	Shadow	Producer's	User's
Pixel-based						
Built area	12	26	16	2	0.8571	0.2143
Surface vegetation	0	23	7	1	0.3382	0.7419
Tree/shrub	2	16	69	5	0.6216	0.7500
Shadow	0	3	19	55	0.8730	0.7143
					Overall	0.6217
					Kappa	0.4781
Object-based						
Built area	12	5	2	0	0.8571	0.6316
Surface vegetation	1	51	4	2	0.7500	0.8793
Tree/shrub	1	11	88	7	0.7928	0.8224
Shadow	0	1	17	54	0.8571	0.7500
					Overall	0.8008
					Kappa	0.7093

sisting of a 256 random stratified per class sample, were used for both assessments.

3. Results

Final results for pixel-based and object-based classifications are found in Figs. 3 and 6, respectively, and a comparison between the two methods is found in Fig. 7. Differences are obvious between the two products: the object-based method is a more spatially cohesive map, with none of the spurious pixel effect found with the pixel-based product. Built areas are also more defined with the object-based method, and accuracy values reflect these differences. The pixel-based classification produced the lowest overall accuracy of 62.11%. Of this overall accuracy, the built area class yielded the lowest accuracy with a user's accuracy of only 21.43%. The other three classes were fair, with user accuracies of 74.19% for the surface vegetation class, 75.00% for the tree/shrub class, and 71.43% for the shadow class.

The object-based classification approach yielded a higher accuracy, with an overall accuracy of 80.08%. This approach also provided higher user accuracy for each LULC class. The built area class had the greatest increase from 21.43% using the pixel-based approach to 63.16% with the object-based approach. The surface vegetation class had the second greatest increase (13.74%) in accuracy using an object-based approach. The tree/shrub and shadow classes increased only moderately with a 7.24% and 3.57% increase, respectively. A pairwise Z-score was

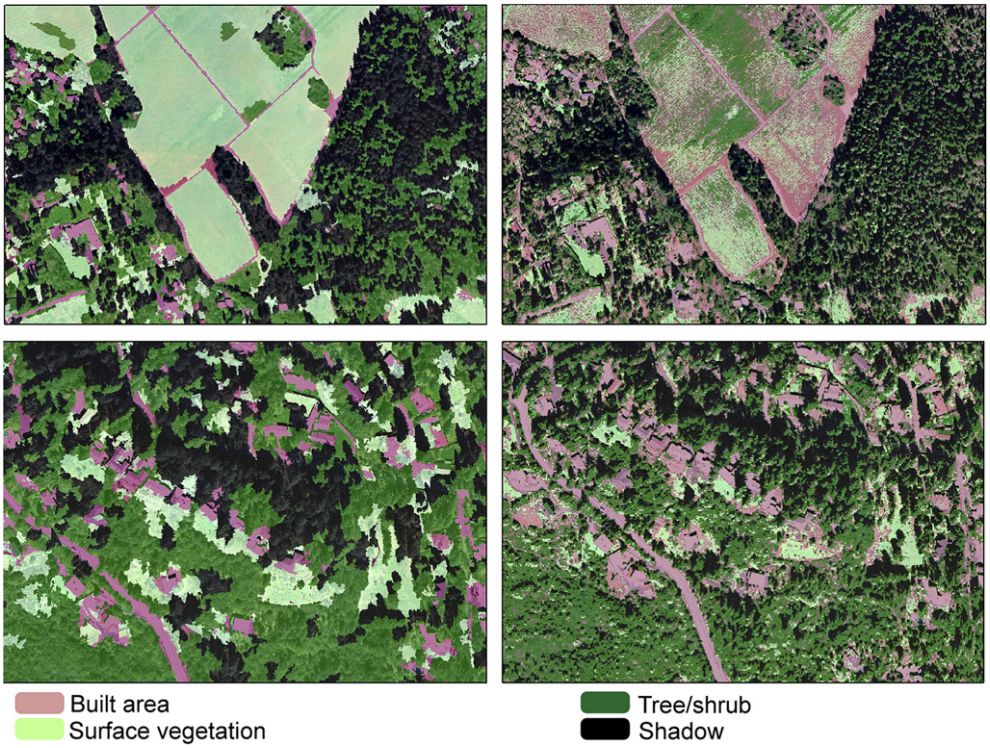

Fig. 7. Comparison of object-based classified map (left) and pixel-based classified map (right). The object-based map delineates features such as structures and yards far better than the pixel-based map.

calculated to compare error matrices, which confirmed that the pixel and object-based error matrices were significantly different (z: 4.2485).

4. Discussion

High-resolution aerial imagery is abundant and freely available for many locations in the US, making it an important resource for scientists, managers, and planners alike. In addition, because recent multi-agency efforts to repeatedly map urban areas in the US with high-resolution imagery fortuitously include the WUI, we can expect more of the same kinds of data to be available. Traditional photointerpretation methods are time- and labor- intensive, expensive, and subjective, making it difficult to fully utilize this valuable data, particularly over large geographic areas. While pixel-based classification methods may be adequate for mapping LULC over large spatial scales, when it comes to classifying detailed land-use types with high-resolution imagery, object-based classification methods may yield better results.

Here, the object-based classification approach provided a 17.97% higher overall accuracy than the pixel-based approach (Fig. 7). This is consistent with other studies that have shown object-based methods out perform pixel-based methods when applied to aerial photographs (Laliberte et al., 2004; Yuan & Bauer, 2006). Here, the object-based approach provided a significantly higher user's accuracy in the built area category with an increase of 41.73%. This was largely due to the better differentiation between the built area class and surface vegetation class using the object-based approach. Using the pixel-based approach, the bulk of the mis-classified surface vegetation is in the fields. Pixels with low texture, and high reflectance, in the absence of spatial context, are classified as urban. The object-based approach recognized contextual values that help differentiate these pixels from urban. In this case, the development of image objects first, rather than pixel by pixel classification, followed by the ability to analyze the relationship between small and large image objects (demonstrated in Fig. 5), resulted in a huge reduction in mis-classification of surface vegetation. The differentiation between built area and surface vegetation is particularly important for wildfire management purposes because mapping structure locations and adjacent fuels is crucial for preventing wildfire-related losses in the WUI. For the purpose of comparing pixel- and object-based approaches, structures were not differentiated from roads here. However, a differentiation could be achieved using topology and shape statistics available with an object-based approach, or by conducting GIS analysis using a roads or parcel layer.

Our results indicate that an object-based classification approach is a more appropriate mapping technique for WUI applications, because it can be used to more accurately distinguish LULC types. In addition, the increase in accuracy that the object-based approach yields for the surface vegetation class is useful for analyzing wildfire threat in WUI areas, because fire movement through surface vegetation can have a different rate of spread and

intensity than fire moving through shrubs and trees (Pyne et al., 1996).

The tree/shrub class yielded similar accuracies using both the pixel-based and object-based approaches, demonstrating that both types of classification methods may be beneficial to land managers and researchers interested in studying urban forests or wildlife species associated with tree and shrub communities. The shadow class also yielded similar accuracies with both methods. Although this class is not particularly useful to land managers, using an object-based approach along with the topological relationships that are built into eCognition, it may be possible to use this class to further differentiate LULC classes. For example, trees are associated with shadow because of their height, and this knowledge may be used to differentiate trees from shrubs.

In addition to the LULC classification results, an additional finding from this study is the importance of spatial enhancements in fuzzy classification methods. Indeed, the spatial enhancement layer was the sole input used to classify the built area class for the large image-object scale – this is the scale at which the majority of the image was classified. The importance of this spatial enhancement is particularly significant because the built area class yielded the greatest accuracy improvement from pixel- to object-based methods. Our results indicate that the use of spatial and spectral enhancements is important to class differentiation.

As we did here, most researchers use standard error matrices (Congalton & Green, 1999; Foody, 2002) to evaluate the accuracy of object-based remotely sensed map products (e.g., Bauer & Steinnocher, 2001; Herold et al., 2003; Kettig & Landgrebe, 1976). However, because object-based classifications generate features with inherent topology in addition to a planimetric map product, assessment of those feature properties can also be envisioned (Hay & Castilla, 2006). For example, the accuracy of the shape and arrangement of features (e.g., homes vis-à-vis surrounding vegetation) might also be assessed. This has not been attempted here, but will be in the future.

The object-based methods presented here could be applied to much larger WUI regions using high resolution satellite or aerial imagery that provides state or national coverage (e.g., National Agriculture Imagery Program (NAIP) aerial imagery for the US and IKONOS Satellite Imagery). These methods are appropriate for any WUI region with moderate tree canopy cover or lower, where structures are visible from above. Field-based mapping methods, while generally more labor intensive and not feasible over large regions, may be more appropriate for WUI regions where structures are frequently obscured by tree canopy.

Across the world, urban areas continue to expand into fire-prone wildland areas. Understanding where the built environment meets wildland areas is important for communities, firefighting personnel, and decision-makers, all of whom can use the maps created with this approach to target areas for wildfire hazard reduction – e.g., vegetation clearing and creating defensible space. In addition, firefighters could use the information to delineate areas that may require special attention (e.g., specific gear or vehicles) during fires.

5. Conclusions

Accurate and timely LULC maps are needed for wildfire management, especially in wildland–urban interface areas where an increasing numbers of homes are being built into wildfire-prone areas. This type of mapped data has useful applications before, during, and after fires happen. Digital image processing is a viable method for producing LULC maps from freely available high-spatial resolution aerial imagery, making it a relatively cost-efficient option. However, it is important to select appropriate image processing techniques to obtain the highest map accuracy possible. Here we have demonstrated that an object-based classification approach yields higher accuracy than a pixel-based classification approach when differentiating between LULC categories in wildland–urban interface areas. An object-based approach more accurately delimited and distinguished between four land-use classes that are necessary building blocks of a fire map product.

References

Alberti, M., Weeks, R., et al. (2004). Urban land cover change analysis in Central Puget Sound. *Photogrammetric Engineering and Remote Sensing, 70*(9), 1043–1052.

Baatz, M., Heynen, M., et al. (2000). eCognition User Guide. Munich, Definiens.

Barlow, J., Franklin, S., et al. (2006). High spatial resolution satellite imagery, DEM derivatives, and image segmentation for the detection of mass wasting processes. *Photogrammetric Engineering and Remote Sensing, 72*(6), 687–692.

Barlow, J., Martin, Y., et al. (2003). Detecting translational landslide scars using segmentation of Landsat ETM^{+} and DEM data in the northern Cascade Mountains, British Columbia. *Canadian Journal of Remote Sensing, 29*(4), 510–517.

Bauer, T., & Steinnocher, K. (2001). Per-parcel land use classification in urban areas using a rule-based technique. *GeoBIT*(6), 12–17.

Benediktsson, J. A., Pesaresi, M., et al. (2003). Classification and feature extraction for remote sensing images from urban areas based on morphological transformations. *IEEE Transactions on Geoscience and Remote Sensing, 41*(9), 1940–1949.

Chubey, M. S., Franklin, S. E., et al. (2006). Object-based analysis of Ikonos-2 imagery for extraction of forest inventory parameters. *Photogrammetric Engineering and Remote Sensing, 72*(4), 383–394.

Cihlar, J. (2000). Land cover mapping of large areas from satellites: status and research priorities. *International Journal of Remote Sensing, 21*(6–7), 1093–1114.

Cohen, J. D. (2000). Preventing disaster: home ignitability in the wildland–urban interface. *Journal of Forestry, 98*(3), 15–21.

Congalton, R. G., & Green, K. (1999). *Assessing the accuracy of remotely sensed data: principles and practices*. Lewis Publishers.

Definiens (2005). eCognition Professional, Munich.

ESRI (2004). ArcGIS software. Environmental Systems Research Institute. Redlands, CA.

Ehlers, M., Gähler, M., et al. (2003). Automated analysis of ultra high resolution remote sensing data for biotope type mapping: new

possibilities and challenges. *ISPRS Journal of Photogrammetry and Remote Sensing, 57*, 315–326.

Foody, G. M. (2002). Status of land cover classification accuracy assessment. *Remote Sensing of Environment, 80*(1), 185–201.

Frontiera, P. L., Kearns, F. R. et al. (submitted for publication). A new approach to assessing parcel-level vulnerability to wildfire in the wildland–urban interface. Landscape and Urban Planning.

Harvey, K. R., & Hill, G. J. E. (2001). Vegetation mapping of a tropical freshwater swamp in the Northern Territory, Australia: A comparison of aerial photography, Landsat TM and SPOT satellite imagery. *International Journal of Remote Sensing, 22*(15), 2911–2925.

Hay, G. J., Blaschke, T., et al. (2003). A comparison of three image-object methods for the multiscale analysis of landscape structure. *Journal of Photogrammetry and Remote Sensing, 57*, 327–345.

Hay, G. J., Castilla, G. (2006). Object-based image analysis: Strengths, weaknesses, opportunities and threats (SWOT). OBIA, 2006: The international archives of the photogrammetry, remote sensing and spatial information sciences, Salzburg, Austria.

Hay, G. J., Marceau, D. J., et al. (2001). A multiscale framework for landscape analysis: object-specific analysis and upscaling. *Landscape Ecology, 16*, 471–490.

Herold, M., Gardner, M. E., et al. (2003). Spectral resolution requirements for mapping urban areas. *IEEE Transactions on Geoscience and Remote Sensing, 41*(9), 1907–1919.

Herold, M., Liu, X. H., et al. (2003). Spatial metrics and image texture for mapping urban land-use. *Photogrammetric Engineering and Remote Sensing, 69*(9), 991–1001.

Hollister, J. W., Gonzalez, M. L., et al. (2004). Assessing the accuracy of national land cover dataset area estimates at multiple spatial extents. *Photogrammetric Engineering and Remote Sensing, 70*(4), 405–414.

Jensen, J. R. (1996). *Introductory digital image processing: a remote sensing perspective*. Upper Saddle River, NJ: Prentice Hall.

Jensen, J. R., & Cowen, D. C. (1999). Remote sensing of urban suburban infrastructure and socio-economic attributes. *Photogrammetric Engineering and Remote Sensing, 65*(5), 611–622.

Kalliola, R., & Syrjänen, K. (1991). To what extent are vegetation types visible in satellite imagery? *Annales Botanici Fennici, 28*, 45–57.

Kelly, M., Shaari, D., et al. (2004). A comparison of standard and hybrid classifier methods for mapping hardwood mortality in areas affected by "sudden oak death". *Photogrammetric Engineering and Remote Sensing, 70*(11), 1229–1239.

Kettig, R. L., & Landgrebe, D. A. (1976). Classification of multispectral image data by extraction and classification of homogeneous objects. *IEEE Transactions on Geoscience and Remote Sensing, 14*(1), 19–26.

Laliberte, A. S., Rango, A., et al. (2004). Object-oriented image analysis for mapping shrub encroachment from 1937 to 2003 in southern New Mexico. *Remote Sensing of Environment, 93*(1–2), 198–210.

Leica (2004). Erdas Imagine 8.7 software.

Liu, D., Kelly, M., et al. (2006). A spatial–temporal approach to monitoring forest disease spread using multi-temporal high spatial resolution imagery. *Remote Sensing of Environment, 101*(2), 167–180.

Murname, R. J. (2006). Catastrophe risk models for wildfires in the wildland–urban interface: What insurers need. *Natural Hazards Review, 7*(4), 150–156.

Pyne, S., Andrews, P., et al. (1996). *Introduction to wildland fire*. New York: John Wiley and Sons.

Radeloff, V. C., Hammer, R. B., et al. (2005). The wildland–urban interface in the United States. *Ecological Applications, 15*(3), 799–805.

Thomas, N., Hendrix, C., et al. (2003). A comparison of urban mapping methods using high-resolution digital imagery. *Photogrammetric Engineering and Remote Sensing, 69*(9), 963–972.

Vogelmann, J., Sohl, T., et al. (1998). Regional characterization of land cover using multiple sources of data. *Photogrammetric Engineering and Remote Sensing, 64*(1), 45–57.

Vogelmann, J. E., Howard, S. M., et al. (2001). Completion of the 1990s National Land Cover Data Set for the conterminous United States from Landsat Thematic Mapper Data and ancillary datasources. *Photogrammetric Engineering and Remote Sensing, 67*, 650–652.

Walsh, S. J., Crawford, T. W., et al. (2001). A multiscale analysis of LULC and NDVI variation in Nang Rong district, northeast Thailand. *Agriculture, Ecosystems and Environment, 85*, 47–64.

Yuan, F., Bauer, M. E. (2006). Mapping impervious surface area using high resolution imagery: A comparison of object-based and per pixel classification. In *American society for photogrammetry and remote sensing annual conference proceedings 2006, Reno, Nevada*.

Yu, Q., Gong, P., et al. (2006). Object-based detailed vegetation classification with airborne high resolution remote sensing imagery. *Photogrammetric Engineering and Remote Sensing, 72*(7), 799–811.

Zhang, Q., Pavlic, G., et al. (2005). A semi-automatic segmentation procedure for feature extraction in remotely sensed imagery. *Computers and Geosciences, 31*(3), 289–296.